Unsteady Outflow of the Vapour into Vacuum from the Flat Surface

German A. Lukyanov

Center for Advanced Studies, St.-Petersburg State Polytechnical University, Polytechnicheskaya Street, 29, 195251, St.- Petersburg, Russia

Abstract. Unsteady expansion of the vapour into vacuum from the flat surface was studied by the direct simulation Monte-Carlo method. The vapour was considered as monatomic gas (the model of hard spheres). The flow structure and parameters in the ranges of flow regimes from free-molecular to continual were investigated.

INTRODUCTION

Unsteady outflow of the vapour (gas) into vacuum from the flat surface is related to a number of classic problems of the rarefied gas dynamics. For the collisionless gas expansion this problem has the self-similar analytical solution [1]. The plane unsteady expansion of the gas into vacuum (the plane rarefaction wave) is the continual analogous to this flow. For the indicated flow in case of the perfect gas the self-similar analytical solution is also known [2]. Generally the expansion of the monatomic gas into vacuum in the presence of collisions is not self-similar and the analytical solution in that case is missing. The problem can be solved by approximate approaches or numerical methods. It was carried out a sufficient amount of this kind of investigations. An important contribution on solution of this problem was made by Cercignani [3], Anisimov [4], Sibold and Urbassek [5, 6], Kelly [7] and a number of other scientists. In the framework of these researches a great attention was given to the flow features in the nonequilibrium Knudsen's layer, the translational relaxation process and other significant properties of the flow. Obtained by now results are commonly used in various applications related to the unsteady expansion of the vapour into vacuum (e.g. pulsed laser ablation of materials). At the same time the present results of computational investigations are not exhaustive on the range of analyzed conditions. It is also required more detailed analysis of common mechanisms of a space-time evolution of a flow structure. In practice of application of the plane unsteady expansion of the gas into vacuum model for the solution of more complex real tasks with nonplanar geometry the mistakes concerned with the incorrect understanding of a number of properties of this flow are often taken place. In this report an attempt to consider this problem in detail and in corpore was made.

NUMERICAL METHOD AND PROBLEM STATEMENT

For the simulation the DSMC method is used (Berd's version [1], NTC – model of hard spheres). The computational domain includes a space between an evaporating surface and an external boundary placed at a sufficient distance from the evaporating surface L. Initial and boundary conditions are formulated as follows. At the initial time moment ($t = 0$) there are no particles in the computational domain ($x > 0$). At $t = 0$ the gas begins to outflow from the evaporating surface ($x = 0$). The velocity distribution function of particles evaporating from the surface at $t > 0$ is supposed to be constant (independent on time) and semi-maxwellian

$$f_e = \frac{n_e}{\left(2\pi R T_w\right)^{3/2}} \exp\left(-\frac{v_x^2 + v_y^2 + v_z^2}{2RT_w} \right), \quad v_x > 0 \,. \tag{1}$$

CP762, *Rarefied Gas Dynamics: 24th International Symposium,* edited by M. Capitelli

Report Documentation Page

Form Approved
OMB No. 0704-0188

1. REPORT DATE	2. REPORT TYPE	3. DATES COVERED
13 JUL 2005	**N/A**	**-**

4. TITLE AND SUBTITLE	5a. CONTRACT NUMBER
Unsteady Outflow of the Vapour into Vacuum from the Flat Surface	5b. GRANT NUMBER
	5c. PROGRAM ELEMENT NUMBER
6. AUTHOR(S)	5d. PROJECT NUMBER
	5e. TASK NUMBER
	5f. WORK UNIT NUMBER
7. PERFORMING ORGANIZATION NAME(S) AND ADDRESS(ES) **Center for Advanced Studies, St.-Petersburg State Polytechnical University, Polytechnicheskaya Street, 29, 195251, St.- Petersburg, Russia**	8. PERFORMING ORGANIZATION REPORT NUMBER
9. SPONSORING/MONITORING AGENCY NAME(S) AND ADDRESS(ES)	10. SPONSOR/MONITOR'S ACRONYM(S)
	11. SPONSOR/MONITOR'S REPORT NUMBER(S)

12. DISTRIBUTION/AVAILABILITY STATEMENT
Approved for public release, distribution unlimited

13. SUPPLEMENTARY NOTES
See also ADM001792, International Symposium on Rarefied Gas Dynamics (24th) Held in Monopoli (Bari), Italy on 10-16 July 2004.

14. ABSTRACT

15. SUBJECT TERMS

16. SECURITY CLASSIFICATION OF:			17. LIMITATION OF ABSTRACT	18. NUMBER OF PAGES	19a. NAME OF RESPONSIBLE PERSON
a. REPORT **unclassified**	b. ABSTRACT **unclassified**	c. THIS PAGE **unclassified**	**UU**	**6**	

Here n_e is the equilibrium vapour concentration, T_w is the surface temperature, v_x, v_y, v_z are the velocity components of particles, R is the gas constant. Particles turning back to the source surface are excluded from the simulation process that corresponds with the condition of their total condensation. Particles reached the external boundary of the computational domain $x = L$ are also excluded from the simulation (the external boundary is supposed to be the condensing surface). The modelling of the gas evaporation into vacuum at such conditions is correct for a hypersonic flow at the external boundary. This requirement was always fulfilled in simulations. For the decreasing of the amount of computations under the realization of DSMC method the distribution function (1) is simulated in the limited range of absolute values of the velocity. The maximum value of velocity components under investigation was $v_m = 4/\beta$, $\beta = (2RT_w)^{-1/2}$. The modelling time corresponded to $\tau = t/t_e \le 10^5$ and the location of the external boundary of the computational domain corresponded to $L \le 10^4 \lambda_e$ (t_e and λ_e – mean time and mean free path defined by equilibrium parameters near the surface). For the simulation the parallel DSMC algorithm [8] was used.

MODELLING RESULTS AND THEIR ANALYSIS

Initial Stage Of Outflow. Free-Molecular And Nearly Free-Molecular Flow Stages

In Fig. 1 the self-similar profiles (dependences on $\xi = \beta x/t$) of relative parameters: velocity βu, density n/n_e, longitudinal T_x/T_w, transverse T_y/T_w and total T/T_w temperatures, flux of particles $\beta un/n_e$ and Mach number M for the collisionless flow as well as the results of calculation of these parameters at $\tau = 10^{-2}$, 10^{-1} and 1 are given. Results obtained practically coincide with each other and with self-similarly profiles for the collisionless gas expansion. Reliable design data are limited by following range $\xi \le 3.2 - 3.4$. Its right boundary is marked with figure *1* (Fig. 1). The flow on this stage is characterized by the rapid density decreasing and the nearly linear increasing of gas velocity while moving away from the surface. The dashed line *2* in Fig.1 corresponds to asymptotic profiles of relative parameters at great values of ξ. The flow is completely translationally nonequilibrium. The transverse temperature T_y is constant. The longitudinal temperature T_x is monotonously decreasing while moving away from the surface. The sonic point (M = 1) corresponds to $\xi = 0{,}337$. Parameters at the sonic point are the following: $\beta u = 0{,}795$, $n/n_e = 0{,}317$, $T/T_w = 0{,}757$, $\beta un/n_e = 0{,}252$.

At $\tau = 1$ the averaged number of collisions of particles under the outflow into vacuum is about 0.1. The value $\tau = 1$ may be assumed as the boundary of the free-molecular stage of the gas outflow. At $\tau = 3$ the number of collisions is increasing up to 1. The influence of collisions on profiles of gasdynamic parameters becomes more appreciable but the difference of design profiles from the self-similar profiles remains insufficient (less 5 – 10 % for T_x and T_y, less 2 – 3 % for u and n). The range $1 < \tau < 3$ may be assumed as the stage of the nearly free-molecular regime. At this stage the transition from collisionless to collisional flow regimes occurs.

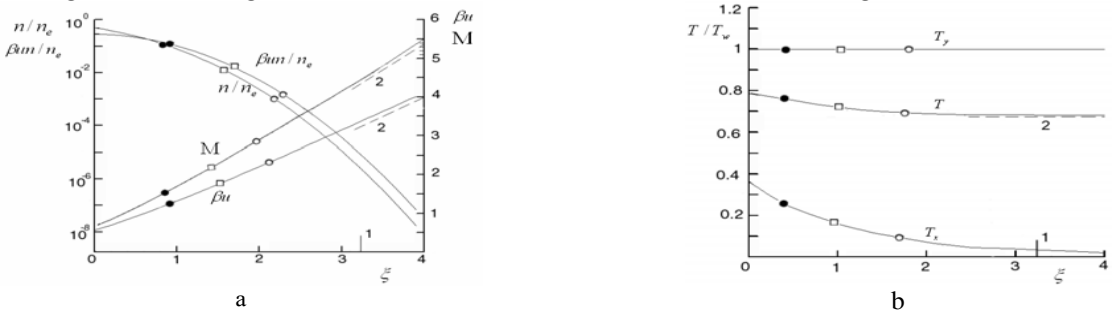

FIGURE 1. Self-similar profiles βu, n/n_e, $\beta un/n_e$, M (a) and T_x, T_y, T (b) at collisionless flow and design results at τ=10^{-2} (•), 10^{-1} (□), 1 (○); 1 – the boundary of the reliable design data region, 2 – asymptotic profiles of parameters at great values of ξ

Transitional And Continual Stages Of Flow Regimes

Let's consider the flow evolution at $\tau \geq 3$. In Fig. 2 profiles βu, n/n_e and $\beta un/n_e$ on coordinate x/λ_e (left) and self-similar coordinate ξ (right) at $\tau = 3$–10 000 are given. There is also presented the self-similar solution for the collisionless flow (curve *0*) in Fig. 2 (right). The origin of design curves in Fig. 2 corresponds to the middle of the first cell ($x = \lambda_e/2$). With the τ growth the flow suffers fundamental changes. It becomes non-self-similar as a whole. This is connected with the appearance of the characteristic scale (mean free path) defining sizes of zones of the translational relaxation. Profiles βu and n/n_e are not self-similar near the surface but they are close to self-similar profiles at sufficiently great ξ. Sizes of the region of the approximate self-similarity of βu and n/n_e are growing with the τ increase. At $\tau > 1000$ the approximate self-similarity of these parameters takes place at $\xi > 0.1$. Profiles $\beta un/n_e$ are approximately self-similar for the whole flow region.

With the τ increase the number of collisions of particles is growing in the gas, the reverse flow of particles to the surface appearing and growing. This results in decreasing βu and increasing n/n_e near the surface. In some zone near the surface the magnitude $\beta un/n_e$ is changed insufficiently (Fig. 2*e*, *f*). At $\tau > 100$ the value of $\beta un/n_e$ near the surface remains approximately constant and equal to 0.24. The 10 % decrease in $\beta un/n_e$ occurs at the distance from the evaporating surface $x/\lambda_e \cong (0{,}3 - 0{,}35)\tau$ or $\xi \cong 0{,}33 - 0{,}4$.

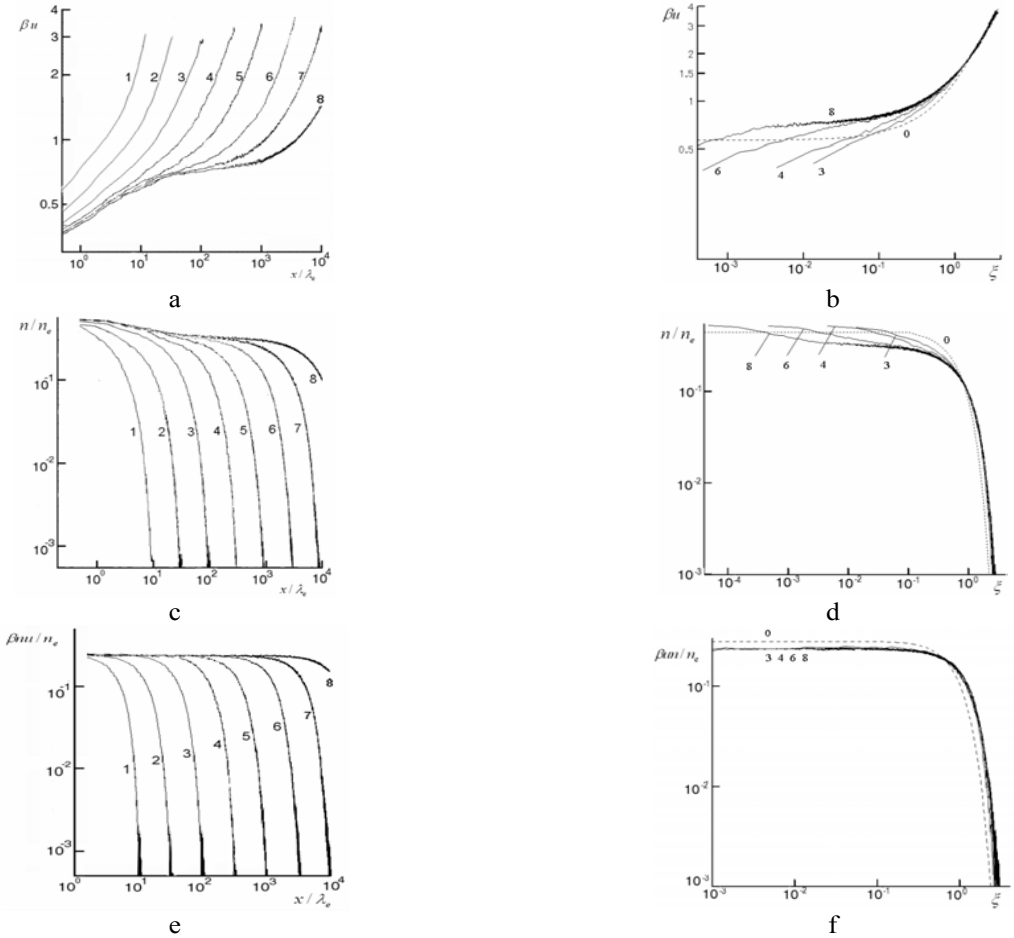

FIGURE 2. Dependences βu, n/n_e and $\beta un/n_e$ on x/λ_e (*a*, *c*, *e*) and ξ (*b*, *d*, *f*) at various time: $\tau = 0$ (curve *0*), 3 (*1*), 10 (*2*), 30 (*3*), 100 (*4*), 300 (*5*), 1000 (*6*), 3000 (*7*), 10000 (*8*)

The governing regularities of this flow are connected with the process of the translational relaxation. In Fig. 3 profiles T_x/T_w and T_y/T_w at $\tau = 30$ (*a*) and 300 (*b*) are given. They represent the course of the translational relaxation with the τ growth. The horizontal line in Fig. 3 corresponds to the value of T_y/T_w at $x \to \infty$. The current position of the gas leading edge is denoted as $x_\phi = 4t/\beta$. At $\tau = 30$ the traslational equilibrium isn't settled due to the insufficient number of collisions. At $\tau > 100$ the zone of the quasi-equilibrium flow is formed at some distance from the surface. Within the bounds of this zone values of T_x and T_y are close, $T_x < T_y$.

The following condition can be assumed as a criterion of the traslational equilibrium

$$\delta = \frac{|T_x - T_y|}{T} \le \varepsilon . \qquad (2)$$

Within the bounds of the Knudsen's layer $\delta > \varepsilon$, at it's external boundary $\delta = \varepsilon$. In Fig. 4 data on the position of the external boundary of the Knudsen's layer x_{Kn} at different τ for $\varepsilon = 0{,}05$ are given. At first at $\tau > 100$ the Knudsen's layer thickness $\Delta_{\text{Kn}} = x_{\text{Kn}}$ sufficiently rapidly decreases and then at $\tau > 1000$ it is changed slightly and approximately equal to $(11 - 12)\lambda_e$. As the time passes parameters at the point x_{Kn} are changed: values of n/n_e and T/T_w increase, βu and M decrease. M number at the external boundary of the Knudsen's layer in the range of $\tau = 10^2 - 10^4$ is changed from 1.48 to 0.775.

The governing regularities of the translational relaxation beyond the bounds of the Knudsen's layer are the following. The magnitude T_x monotonously decreases and the curve T_y has its minimum. The minimum's coordinate x_m is moving away from the surface with the τ growth. The dependence $x_m(\tau)$ (Fig. 4) at $\tau \ge 30$ can be approximated by

$$x_m/\lambda_e = 0{,}67\tau^{1{,}16}, \quad \xi_m = 1{,}12\frac{x_m}{\tau\lambda_e} = 0{,}75\tau^{0{,}16}. \qquad (3)$$

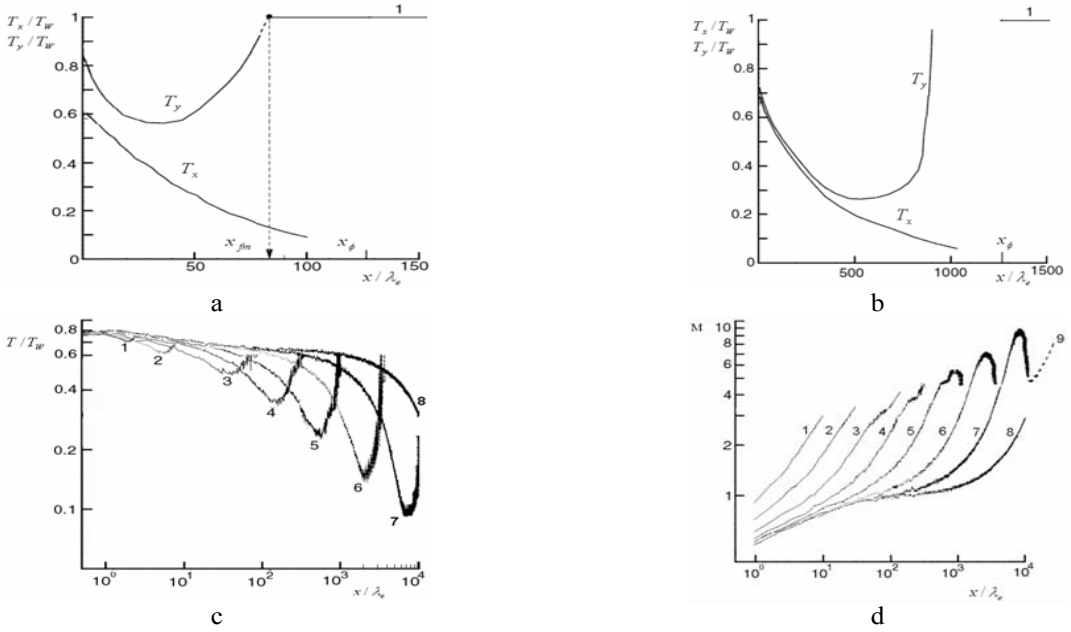

FIGURE 3. Dependences T_x/T_W (a, b), T_y/T_W (a, b), T/T_W (c) and M (d) on x/λ_e at various time: a - τ=30, b - τ=300, c and d - τ=3 (*1*), 10 (*2*), 30 (*3*), 100 (*4*), 300 (*5*), 1000 (*6*), 3000 (*7*), 10000 (*8*)

At $x > x_m$ the value of T_y rapidly increases approaching to the value of $T_y/T_w = 1$ corresponding with the free-molecular mode of the flow. Such behavior of curves T_y is accounted for particles practically collisionless moving

in the region adjoining to the gas leading edge. This feature of changing T_y at $x > x_m$ can be used for the determination of the boundary of the flow transition to the free-molecular mode of the expansion. As such boundary we shall consider the intersection of the design curve T_y linearly extended (the dashed line in Fig. 3*a*) with the line $T_y / T_w = 1$. Let's denote this point as x_{fm}. The dependence $x_{fm}(\tau)$ is given in Fig. 4. Design data at $\tau \geq 30$ are approximated by:

$$x_{fm} / \lambda_e = (2{,}9 - 3{,}2)\tau, \quad \xi_{fm} = 3{,}2 - 3{,}5 . \tag{4}$$

Regularities of T_x and T_y changes identically determine profiles *T*. The typical feature of the *T* profiles is the presence of the minimum at the point x_m and the tendency of T to the value $T = 0{,}67T_w$ in the region of the free-molecular expansion ($x > x_{fm}$). Profiles u and T define Mach number profiles. The presence of the *T* minimum results in appearing the local maximum of the M profile at the point x_m at $\tau > 100$ (Fig. 3*d*). M number at the local maximum point is increasing with the τ growth. Simulations carried out describe the flow in the region $\xi \leq 3{,}2 - 3{,}4$. It was shown above $M \sim x / t$ for the free-molecular region of the gas expansion. The hypothetical form of the M profile at $x > x_m$ for $\tau = 3000$ is given in Fig. 3*d* (dotted line *9*).

At $\tau > 100$ the form of gasdynamic parameters profiles (Fig. 2 and 3) points out the formation of two flow regions with the distinction in kind of regularities of parameters changes: the subsonic quasi-steady region with the thickness Δ_* and the supersonic flow region Δ_s downstream located (Fig. 4). Both regions have the fairly complex internal structure. In Fig. 4 data on the sonic point location (M = 1) are presented while in Fig. 8 parameters at this point are given. The coordinate of the sonic point x_* is monotonously increasing with the τ growth. At $\tau > 30$ dependences x_* / λ_e and ξ_* on τ can be approximated by

$$x_* / \lambda_e = \tau^{0{,}575}, \quad \xi_* = 1{,}12\tau^{-0{,}425}. \tag{5}$$

At $\tau = \tau_b \cong 200$ (Fig. 4) values of x_{Kn} and x_* are equal. At $\tau > \tau_b$ the external boundary of the Knudsen's layer is located in the region of the subsonic flow. In the range $100 < \tau < \tau_b$ we have $x_{\mathrm{Kn}} > x_*$. Within the bounds of this short interval τ the flow at the sonic point is nonequilibrium. At the sonic point at $\tau = 30 - 10\,000$ (Fig. 5) parameters n_* / n_e, βu_* and T_* / T_w are changed slightly (especially at $\tau \geq 1000$). This feature can be used for the approximate statement of boundary conditions at the surface under the present problem solution by the continual gasdynamic approaches (Euler or Navier – Stokes equations).

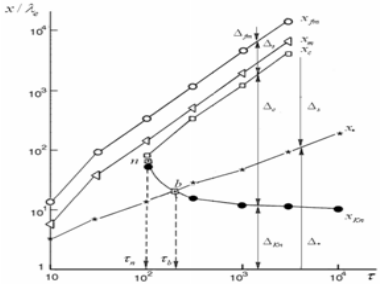

FIGURE 4. Gasdynamic structure of the flow at transitional and continual stages at coordinates x / λ_e, τ

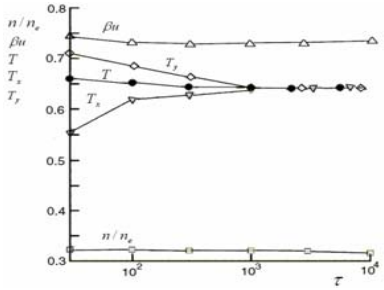

FIGURE 5. Parameters at the sonic point of the flow

The flow in the subsonic region is characterized by the fairly rapid decrease of gradients of gasdynamic parameters with the x increase (Fig. 2 and 3). With the τ growth this tendency is gaining strength. At the stage of the developed continual regime ($\tau > 1000$) in the subsonic region the zone of the rapid acceleration of the gas up to M = 0,8 – 0,9 with the extension (20 – 30) λ_e and the transonic zone with the much great extension can be pointed out. The size of the transonic zone is growing with the τ increase. Downstream the supersonic unsteady region is located. Within the bounds of this region the rapid growth of βu, decrease of n / n_e and $\beta u n / n_e$ are observed.

At $\tau > 100$ downstream from the Knudsen's layer the region of the continual (quasi-equilibrium) flow is located. The extension of this zone is growing with the τ increase. As an external boundary of the continual region can be

assumed the coordinate x_c where condition (2) is true. The location $x_c(\tau)$ at $\varepsilon = 0{,}05$ is presented in Fig. 4. The extension of the region of the continual flow is equal to $\Delta_c = x_c - x_{\mathrm{Kn}}$. At some magnitude $\tau = \tau_n$ the external boundary of the region of the continual flow x_c is confluent with the external boundary of the Knudsen's layer x_{Kn} (Fig. 4). At $\varepsilon = 0{,}05$ we have $\tau_n \cong 100$. At $\tau < \tau_n$ the Knudsen's layer as a zone of the relaxation of the initial nonequilibrium cannot be assumed since the flow located left from the point *n* is nonequilibrium in the whole region. Above the line x_{fm} the region of the free-molecular flow is located. Between the lines x_{fm} and x_c the region of the transitional regime of the flow is located. Its size $\Delta_t = x_{fm} - x_c$ is growing with the τ increase.

GENERALIZED GASDYNAMIC STRUCTURE AT COORDINATES ξ, τ

The summarizing of design data allows to represent the time evolution of the gasdynamic structure for the flow as a whole (Fig. 6). At coordinates ξ, τ the whole flow field can be divided into three regions: free-molecular *F*, transitional *T* and continual *C* flows. At $\tau > 3$ the region of the free-molecular regime has two subregions: the first one is located above the line *rf* corresponding to the boundary of the free-molecular regime ξ_{fm}, the second one is placed below the line *rp* corresponding to the boundary of the vapour layer ξ_{fw} with the thickness $x = \lambda_e$ adjoining to the evaporating surface. Left from the point *r* ($\tau < 3$) the flow is completely free-molecular or nearly free-molecular. The region of the transitional regime is located between the lines *prf* and *knc*. The line *knc* divides the transitional flow from the continual one. It consists of the external boundary of the Knudsen's layer ξ_{Kn} and the distant boundary of the region of the continual flow ξ_c. Right from the line *knc* the region *C* is located.

The time evolution of the gasdynamic structure of the flow has four typical stages (Fig. 6): *1* — free-molecular ($\tau < 1$), *2* — nearly free-molecular ($1 < \tau < 3$), *3* — transitional ($3 < \tau < 100$) and *4* — continual ($\tau > 100$). Here and above names of flow stages correspond to names of mostly dense flow regimes realized at the corresponding stage. At stages *1* and *2* the flow regime *F* takes place. At stage *3* the flow includes the region of the transitional regime *T* ($\xi_{fw} < \xi < \xi_{fm}$) and two zones of the region *F* ($\xi < \xi_{fw}$ and $\xi > \xi_{fm}$). At the forth (continual) stage the flow includes regions with three flow regimes.

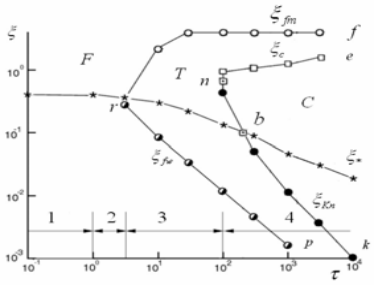

FIGURE 6. Generalized gasdynamic structure of the flow at coordinates ξ, τ

The Knudsen's layer ($\xi < \xi_{\mathrm{Kn}}$) including the free-molecular sublayer ($\xi < \xi_{fw}$) and the zone of the transitional flow ($\xi_{fw} < \xi < \xi_{\mathrm{Kn}}$) is placed near the surface. Farther the regions of continual ($\xi_{\mathrm{Kn}} < \xi < \xi_c$), transitional ($\xi_c < \xi < \xi_{fm}$) and free-molecular ($\xi > \xi_{fm}$) flows are located.

REFERENCES

1. G.A. Bird, Molecular gas dynamics and direct simulation of gas flows, Clarendon Press, Oxford, 1994, 451 p.
2. G.G. Cherniy, Gas dynamics, Nauka, Moscow, 1988, 424p.
3. C. Cercighani, in Rarefied Gas Dynamics, edited by S.S. Fisher, AIAA, New York, 1981, pp. 305-320.
4. S.I. Anisimov, Soviet Physik JETP, **27**, 182-185 (1968).
5. D. Sibold and H.M. Urbassek, Phys. Rev. A, **43**, 6722 –6734 (1991).
6. D. Sibold and H.M. Urbassek, Phys. Fluids A, **5**, 243-255 (1993).
7. R. Kelly, Phys. Rev. A, **46**, 860-874 (1992).
8. Y.Yu. Bykov, Yu.E. Gorbachev and G.A. Lukyanov, Thermophys. and Aeromech., **5**, 399-405 (1998).